• Original Paper •

Precipitation Controls on Carbon Sinks in an Artificial Green Space in the Taklimakan Desert

Yingwei SUN^{1,2}, Fan YANG¹, Jianping HUANG³, Xinqian ZHENG⁴, Ali MAMTIMIN¹, Chenglong ZHOU¹, Silalan ABUDUKADE¹, Jiacheng GAO¹, Chaofan LI⁵, Mingjie MA¹, Wen HUO¹, and Xinghua YANG¹

¹Institute of Desert Meteorology, China Meteorological Administration/National Observation and Research Station of Desert Meteorology, Taklimakan Desert of Xinjiang/Taklimakan Desert Meteorology Field Experiment Station of China Meteorological Administration/Xinjiang Key Laboratory of Desert Meteorology and Sandstorm/Key Laboratory of Tree-ring Physical and Chemical Research, China Meteorological Administration, Urumqi 830002, China ²Xinjiang Branch of China Meteorological Administration Meteorological Cadre Training College, Urumqi 830002, China ³Collaborative Innovation Center for Western Ecological Safety, College of Atmospheric Sciences, Lanzhou University, Lanzhou 730000, China

⁴Xinjiang Agro-Meteorological Observatory, Urumqi 830002, China

⁵Collaborative Innovation Center on Forecast and Evaluation of Meteorological Disaster, School of Geographic Sciences, Nanjing University of Information Science and Technology, Nanjing 210044, China

(Received 3 January 2023; revised 8 April 2024; accepted 21 May 2024)

ABSTRACT

Control of desertification can not only ameliorate the natural environment of arid regions but also convert desertified land into significant terrestrial carbon sinks, thereby bolstering the carbon sequestration capacity of arid ecosystems. However, longstanding neglect of the potential carbon sink benefits of desertification management, and its relationship with environmental factors, has limited the exploration of carbon sequestration potential. Based on CO_2 flux and environmental factors of artificial protective forest in the Taklamakan Desert from 2018 to 2019, we found that the carbon storage capacity of the desert ecosystem increased approximately 140-fold after the establishment of an artificial shelter forest in the desert, due to plant photosynthesis. Precipitation level sess than 2 mm had no impact on carbon exchange in the artificial shelter forest, whereas a precipitation level of approximately 4 mm stimulated a decrease in the vapor pressure deficit over a short period of about three days, promoting photosynthesis and enhancing the carbon absorption of the artificial shelter forest. Precipitation events greater than 8 mm stimulated soil respiration to release CO_2 and promoted plant photosynthesis. In the dynamic equilibrium where precipitation stimulates both soil respiration and photosynthesis, there is a significant threshold value of soil moisture at 5 cm $(0.12 \text{ m}^3 \text{ m}^{-3})$, which can serve as a good indicator of the strength of the stimulatory effect of precipitation on both. These results provide important data support for quantifying the contribution of artificial afforestation to carbon sequestration in arid areas, and provide guidance for the development and implementation of artificial forest management measures.

Key words: Taklimakan Desert, artificial shelter forest, carbon sequestration capacity, CO₂ flux, precipitation

Citation: Sun, Y. W., and Coauthors, 2024: Precipitation controls on carbon sinks in an artificial green space in the Taklimakan desert. *Adv. Atmos. Sci.*, **41**(12), 2300–2312, https://doi.org/10.1007/s00376-024-3367-8.

Article Highlights:

- $\bullet \ \ Establishing \ artificial \ protective \ forests \ in \ the \ desert \ increases \ the \ carbon \ sink \ capacity \ of \ desert \ ecosystems.$
- The carbon sink capacity and duration of artificial protective forests are significantly correlated with precipitation level.
- When precipitation exceeds 8 mm, a clear threshold reflects its stimulation intensity on soil respiration and photosynthesis.

1. Introduction

Desertification has become a significant global environmental and socioeconomic issue in many countries world-

^{*} Corresponding author: Fan YANG Email: yangfan@idm.cn

wide. Desertification is not solely a natural phenomenon, but is intricately connected to environmental, economic, and social development, as the outcome of complex interactions between various natural, biological, political, social, cultural, and economic factors (Lal, 2004; Martínez-Valderrama et al., 2016; Liang et al., 2021). Numerous factors contribute to desertification, with the primary cause being the harsh natural environment in arid regions, closely followed by human activities that impose stress on the delicate ecological settings of these vulnerable regions. Human activity is a significant driver of the occurrence and progression of desertification. Thus, humans are both the main catalyst and primary sufferers of desertification (Reynolds et al., 1999, 2007; Lal, 2004; Wijitkosum, 2021). Desertification has affected a quarter of the global land area, with 10%–20% of drylands experiencing degradation, as described by the 1994 Convention to Combat Desertification, directly impacting approximately 250 million individuals, mostly in developing nations. In the face of global climate change and population growth, desertification is predicted to gradually intensify in the future (Reynolds et al., 2007; Huang et al., 2016a, 2016b, 2017, 2019).

It is estimated that desertification causes both significant direct economic losses and historical global carbon losses, ranging from 20 to 30 Pg. Assuming that two-thirds of the historical carbon loss can be utilized, the potential for organic carbon sequestration within 50 years could reach 12-20 Pg (Lal, 2004). Approaches to land use and management for increasing organic carbon sequestration include afforestation with suitable species, farmland soil management, pasture management, and the restoration of degraded soils and ecosystems through afforestation and conversion to other restorative land uses (Duan et al., 2001; Lal, 2004; Zhang and Huisingh, 2018). The estimated potential of global soil organic carbon sequestration is approximately 1 Pg C yr⁻¹ (Lal, 2004). Therefore, the control of desertification would improve the regional ecological environment and convert desertified land into a significant terrestrial carbon sink (Ai et al., 2018), representing a crucial step in consolidating and improving the carbon sink capacity of ecosystems in arid areas. Desertification control is also an economical and reliable approach for slowing or delaying global warming. However, to date, most research attention has focused on the roles of wind erosion prevention, sand fixation, microclimate improvement, and potential economic benefits associated with the control of desertification. The potential carbon sink benefits have been overlooked for a considerable time (Ma et al., 2021).

In recent years, China has successfully implemented several national key ecological projects, including the control of wind and sand in Beijing and Tianjin, the conversion of farmland to forest and grassland, the Three-North Shelterbelt Program, and the comprehensive control of rocky desertification. These projects have led to a historic change from "sand advancing/people retreating" to "green advancing/ sand retreating". Afforestation and reforestation play crucial roles in combating desertification, and are also the most cost-effective means of increasing the carbon storage of

desert ecosystems and slowing the increase in atmospheric CO₂ concentration (Hastings et al., 2005; Zhang et al., 2009; Xu et al., 2019; Wang and Huang, 2020; He et al., 2021). As of 2016, an artificial Haloxylon ammodendron forest in the Hexi Corridor covered an area of 89 000 ha. The earliest and largest artificial H. ammodendron forest was established in Mingin County, with a preserved area of 43 500 ha. This forest plays a crucial role in improving the microclimate, enhancing soil quality, protecting biodiversity, and increasing the carbon sink. It has been estimated that each square meter of the artificial H. ammodendron forest ecosystem fixes 434 g C yr⁻¹ (Ma et al., 2021). However, compared to other regions, the harsh environments in arid areas, with sparse precipitation, strong evaporation, and frequent sandstorms, makes the effectiveness of afforestation in enhancing carbon sequestration very uncertain. Therefore, understanding the carbon sequestration process in artificial forests and its relationship with environmental factors is fundamental to objectively evaluating its carbon sequestration potential and formulating effective management measures.

The Taklimakan Desert is the second largest shifting desert worldwide; it is situated in the arid region of Northwest China. To meet human needs, especially for oil extraction in desert areas, many artificial green spaces have been established in desert areas to resist wind and sand exposure and provide comfortable environmental conditions for the internal core area. From the outside to inside, the structure of this artificial green land is a grass checkerboard sand barrier, artificial shelter forest through artificial drip irrigation, and internal production and living areas. The main species planted in artificial shelter forests include Tamarix ramosissima, H. ammodendron, and Calligonum arborescens (Lei et al., 2008; Wang et al., 2008). Previous studies have indicated that the desert ecosystem can store CO₂ through abiotic processes, with the carbon sink capacity providing an average annual CO₂ absorption of 7.11 g m⁻² yr⁻¹ (Yang et al., 2020a). Furthermore, artificial shelter forest establishment has altered the original abiotic carbon sequestration process of the desert, enhancing carbon sequestration through photosynthesis, soil improvement, and biodiversity promotion. Arid regions of Northwest China, including the Taklimakan Desert, have experienced significant warming and increased humidity due to global climate change. These changes are manifested through increases in total precipitation and extreme rainfall events (Shen et al., 2010; Donat et al., 2017; Yao et al., 2020; Zhang et al., 2021b), which have affected nutrient and water availability in desert soil; the increased amount of precipitation penetrating the soil also affects plant roots and soil microorganisms. Alterations to precipitation patterns will inevitably impact the carbon sequestration potential of artificial shelter forests in desert environments, involving many processes such as photosynthesis, root depth distribution in desert vegetation, and soil respiration stimulation (Cable et al., 2004; Midgley et al., 2004; Yang et al., 2020b, 2022; Zhang et al., 2021a). However, we still lack a systematic understanding of the responses of these processes to differing levels of precipitation in desert environments, leading to many uncertainties in the accurate quantification of the carbon sequestration capacity of artificial afforestation in deserts and the exploration of its carbon sequestration potential.

In this study, we used an eddy covariance approach to monitor CO₂ flux and multiple environmental factors in the artificial shelter forest located in the hinterland of the Taklimakan Desert in 2018 and 2019, to analyze the enhancement of the desert carbon sequestration capacity by the establishment of artificial shelter forest and its response mechanism to different magnitudes of precipitation events. The objective of this study was to enhance our understanding of the carbon cycle in desert ecosystems and contribute to the development and implementation of management strategies for artificial forests in deserts. Additionally, this study provides data support for quantifying the contribution of artificial afforestation in arid regions to carbon sequestration and sink enhancement.

2. Materials and methods

2.1. Site description

The Taklimakan Desert is situated in the center of the Tarim Basin in the Xinjiang Uygur Autonomous Region, China, and covers a total area of 337 600 km². It is the second

largest shifting desert worldwide, with approximately 70% of its area covered by shifting sand, and is a significant source of dust aerosols to the global atmosphere (Lei et al., 2008; Li et al., 2015; Yang et al., 2021). The observation station was located in an artificial shelter forest surrounding the National Observation and Research Station of Desert Meteorology, Taklimakan Desert of Xinjiang (38°58' N, 83°39'E, 1099 m MSL) in the hinterland of the Taklimakan Desert (Fig. 1). The entire desert hinterland has an arid desert climate within a warm temperate zone, with an average annual precipitation of only 25.9 mm, which is primarily distributed between May and August. In recent years, due to gradual warming and increasing rainfall in Northwest China, both the overall precipitation amount and likelihood of rainstorms within the Taklimakan Desert have seen an upswing (Li et al., 2016). The annual potential evaporation is 3812.3 mm, which is almost 150 times the average annual precipitation. Seasonal changes in the study area are significant, and significant temperature fluctuations occur between day and night. The average annual temperature is 12.1°C, with maximum temperatures ranging as 40.0°C-46.0°C, and minimum temperatures dropping as low as -20.0°C to -32.6°C. The prevailing easterly winds maintain an average annual speed of 2.3 m s⁻¹. The extensive presence of sand on the surface acts as source material for dust and sand

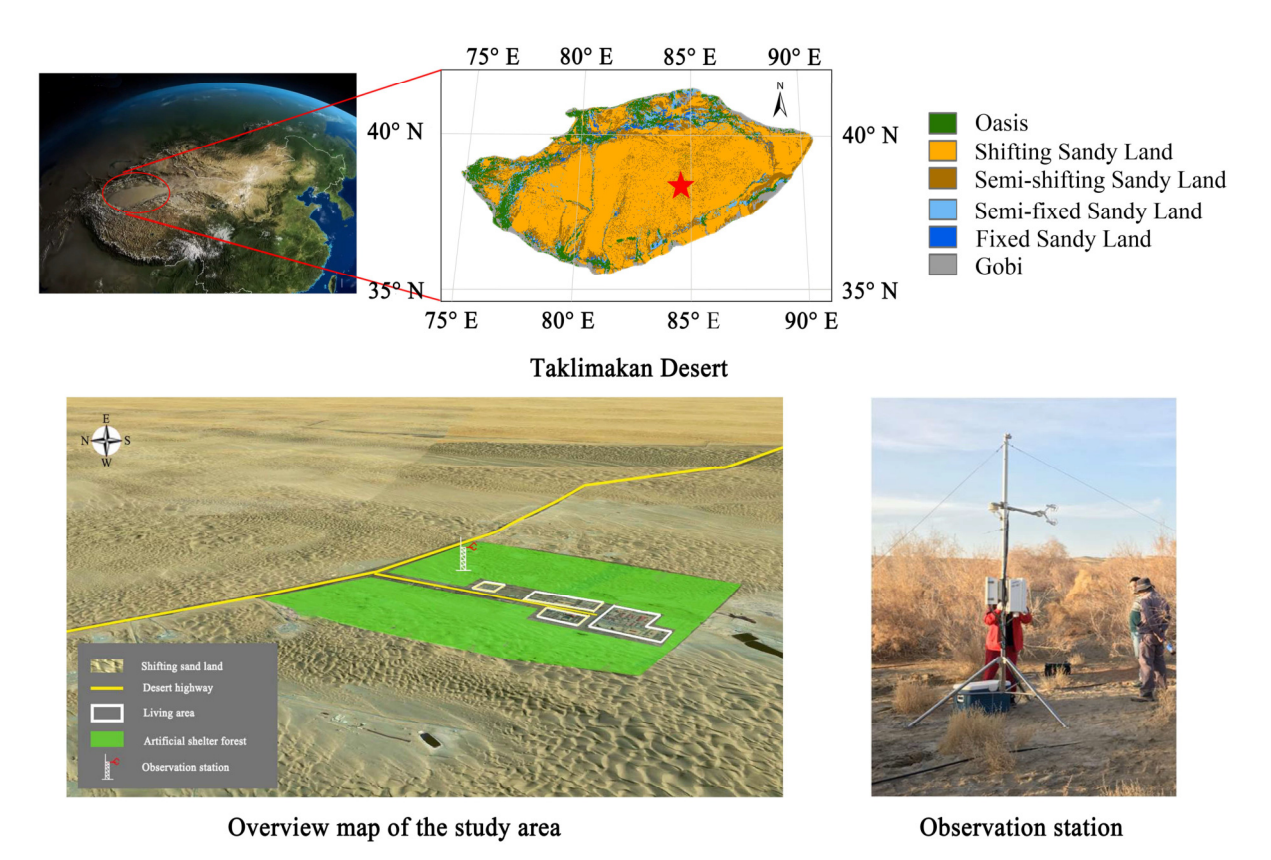


Fig. 1. Upper panels: Distribution of land-cover types in the Taklimakan Desert, indicating the location of the National Observation and Research Station of Desert Meteorology, Taklimakan Desert of Xinjiang (red star). Lower panels: Overview of the artificial shelter forest in the hinterland of the Taklimakan Desert (left) and positioning of the observation station (right).

storm weather. Floating dust and blowing sand occur for over 157 days on average annually, and sandstorms occur on 16 days each year (Lei et al., 2008; Li et al., 2015; Yang et al., 2017). The desert's extreme harsh environmental conditions have resulted in a lack of natural vegetation cover within the region. In the 1990s, to ensure the exploitation of desert oil, a series of artificial shelter forests were established in the Taklimakan Desert, which were mainly composed of *T. ramosissima*, *H. ammodendron*, and *C. arborescens*, and cultivated by artificial drip irrigation. The shelter forest around the observation station has a square shape and covers an approximate area of 3.6 km², with an average height of 1.5 m.

2.2. Experimental design

In November 2017, an open-path eddy covariance system (height: 3 m) was deployed in a green space 300 m from the northeast boundary of the artificial shelter forest (Table 1) to gauge the exchange of energy, CO₂, and H₂O between the land and atmosphere in the artificial shelter forest. Simultaneously, soil CO₂ flux is continuously monitored every 0.5 h using an automatic soil CO₂ flux measurement system. Two layers of sensors are buried in the soil to measure soil temperature and moisture. All sensors are consolidated on a CR1000 data collector (Campbell Scientific, Logan, UT, USA). Further details regarding the instruments used in the experiment are given in Table 1. All time references in this study refer to local time (LT), which is 2 h and 25 min later than Beijing time.

2.3. Data processing and statistical analyses

The collected flux and meteorological data were processed into 30-min intervals using the EasyFlux PC software (Campbell Scientific). Abnormal data caused by equipment failure, equipment maintenance, precipitation, and human factors were eliminated. Gaps in the data were filled using the average daily change method (Falge et al., 2001) and interpolation (Aubinet et al., 2002; Baldocchi, 2003). Precipitation data were obtained from an automatic tipping bucket rain gauge, located 200 m from the observation station.

The Origin 2019b software was used to perform statistical analysis on the data from 2018 to 2019. First, the distribution of precipitation magnitudes during the main plant growth seasons during the observation period was statistically analyzed to identify precipitation patterns and assist with

the classification of subsequent precipitation events. Next, we performed regression analysis between the total daily CO₂ exchange of the artificial shelter forest and variation in precipitation amounts to understand the impact of precipitation events of different magnitudes on the CO₂ flux of the artificial shelter forest. For continuous precipitation over multiple days, the consecutive days were combined and treated as a single precipitation event. In order to minimize the interference from other variables (such as irrigation) during the study of the impact of precipitation, thereby ensuring the accuracy and reliability of the research results, we removed data collected during and after the drip irrigation period when analyzing the carbon dioxide exchange in artificial shelter forests. Finally, representative precipitation events were selected to compare the CO₂ exchange in the artificial shelterbelt forests with the seven days following precipitation. On this basis, the degree of impact of different magnitude precipitation events on the total daily CO₂ exchange of artificial shelterbelt forests were analyzed, and their trends and duration of effects were also assessed.

3. Results and discussion

3.1. Meteorological conditions

The meteorological conditions within the artificial shelter forest during the observation period are shown in Fig. 2. Throughout the observation period, there were significant seasonal temperature fluctuations, with an average temperature of 11.88°C, maximum temperature of 43.42°C, and minimum temperature of -26.2°C. The atmospheric pressure ranged from 86.14 to 91.03 KPa, with a recognizable seasonal pattern. The annual variation of vapor pressure showed the opposite trend to that in temperature, with the lowest values in summer, followed by spring, autumn, and in winter. The average relative humidity was 34.94%. Within the study area, the average wind speed for each half-hour interval was 1.24 m s⁻¹, with a maximum wind speed of 6.64 m s⁻¹. The wind speed increased significantly during spring, which was the main period for sandstorm outbreaks. Variation in soil temperature during the observation period was consistent with the trends in air temperature. The average temperature of the surface soil was 13.09°C, with a maximum of 66.57°C and a minimum of -24.95°C. Throughout the observation period, 13 and 20 precipitation events were recorded

Table 1. Summary of the instruments used in the experiment from November 2017 to December 2019.

Observation system	Variables	Time interval	Sensor	Height/depth (m)
Eddy covariance system	Three-dimensional wind speed and direction, Ta, RH, CO ₂ /H ₂ O concentration, H, LE, u*, FC	IRGASON (Campbell Scientific)	3	
Air temperature, humidity	Ta and RH	30 min	HMP155A (Vaisala)	3
Soil respiration	Rs	30 min	LI-8100A (LI-COR)	0.0
Soil temperature Soil moisture	Soil temperature gradient Soil moisture gradient	30 min 30 min	109 (Campbell Scientific) 93640 Hydra (Stevens)	0.0, -0.05, -0.1 -0.05, -0.1

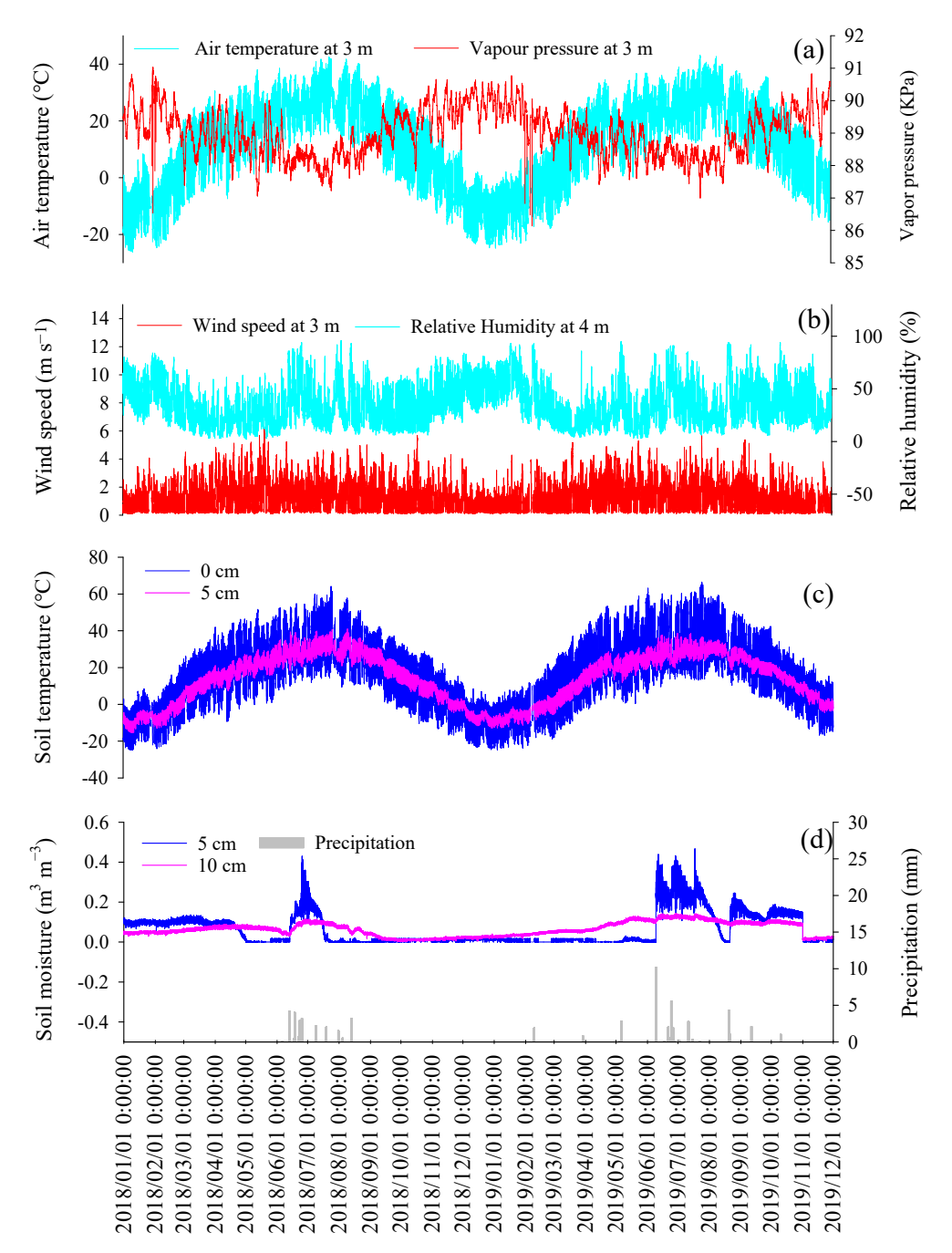


Fig. 2. Meteorological conditions in the study area at 30-min intervals during the observation period: (a) air temperature and pressure at 3 m above the surface; (b) wind speed at 3 m and relative humidity at 4 m above the surface; (c) temperature at the soil surface and 5 cm depth; (d) precipitation and soil moisture at depths of 5 and 10 cm.

in 2018 and 2019, respectively, primarily occurring in June and July. The total precipitation for the corresponding time-frames was only 27.4 and 38.1 mm, respectively (Fig. 3). The majority (96.9%) of recorded precipitation events contained < 6 mm of rainfall. Among the numerous precipitation events, a rare high-precipitation event (total: 10.2 mm) occurred on 9 June 2019.

3.2. Temporal variation of the CO_2 flux

The CO2 flux data for the non-vegetated shifting sand

area in the study area are shown in Fig. 4; these are based on the CO_2 flux calculation scheme established by Yang et al. (2020a, 2023). Compared to the CO_2 budget of non-vegetated shifting sand, the artificial shelter forest showed significant CO_2 absorption during the day and CO_2 release at night. The highest absorption peak was -11.67 µmol m⁻² s⁻¹, which occurred at noon on 7 June 2018. We found that the carbon storage capacity of the desert ecosystem increased approximately 140-fold after the establishment of an artificial shelter forest in the desert, due to plant photosynthesis

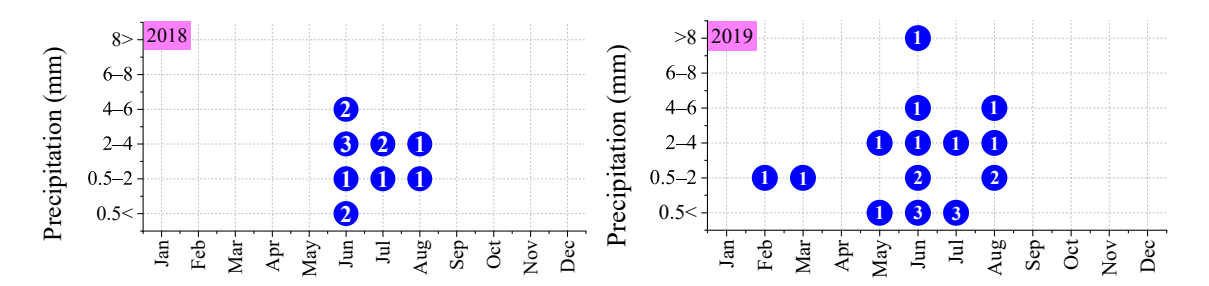


Fig. 3. Distribution of precipitation events' different magnitudes in the study area during the observation period. Numbers in blue circles are numbers of precipitation events.

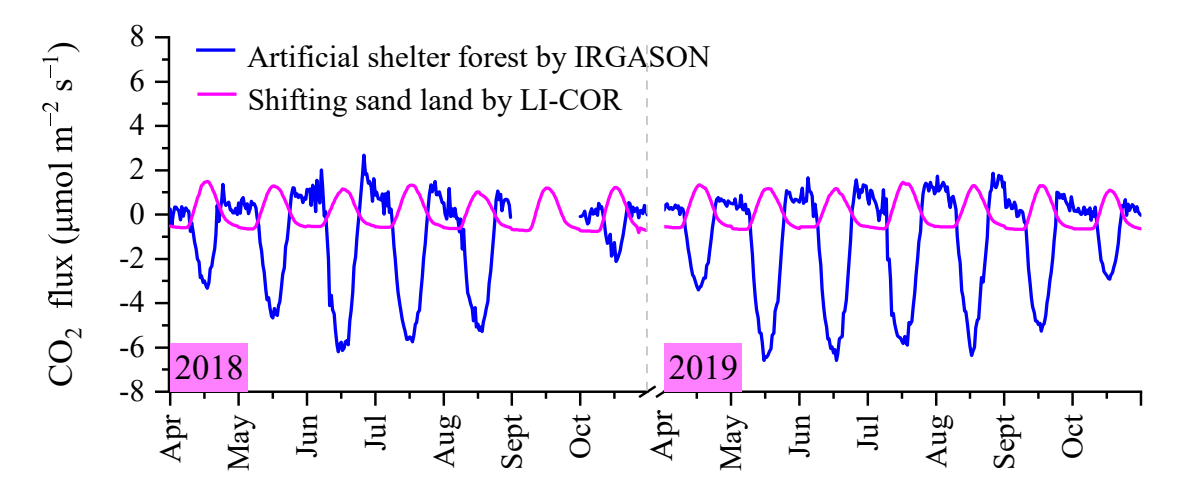


Fig. 4. Comparison of the monthly mean diurnal variation in CO_2 flux between the artificial shelter forest and non-vegetated shifting sand in the study area during the growing season. Observation data for the artificial shelter forest were lost in September 2018 due to a loss of power supply.

 $(-1000 \text{ g m}^{-2} \text{ yr}^{-1} \text{ vs.} -7.11 \text{ g m}^{-2} \text{ yr}^{-1})$ (Yang et al.,2020a). The establishment of the artificial shelter forest on shifting sand completely covered the processes of the inorganic CO₂ budget dominated by soil air expansion/contraction and saline alkali chemical carbon sequestration caused by soil heat fluctuation in the shifting sand (Yang et al., 2020a). Additionally, CO₂ flux varied significantly in the artificial shelter forest during the growing season, due to plant growth regulation. The artificial shelter forest had a relatively robust carbon sequestration effect during the vigorous vegetation growth period in summer. Overall, the establishment of the artificial shelter forest successfully compensated for the relatively weak CO₂ budget process of the shifting sand, and there was a notable carbon sequestration effect during the growing season. These findings were consistent with those of previous studies on the carbon sequestration capacity of artificial forests in the Three-North Shelterbelt Program, alpine sandy shrub forest on the Qinghai-Tibet Plateau, H. ammodendron plantations in the Shiyang River Basin, and the mixed plantation in the dry hot valley of the Jinsha River (Liu et al., 2014; Gong et al., 2019; He et al., 2021; Ma et al., 2021). Table 2 shows the amounts of CO₂ sequestration achieved by the artificial shelter forest throughout the growing season, which reached approximately 1000 g m⁻² yr⁻¹. This value was significantly higher than that of the artificial H. ammodendron forest in the Shiyang River Basin (140 g m⁻² yr⁻¹), artificial fixed vegetation in the Tengger Desert (81.9 g m⁻² yr⁻¹), and the Inner Mongolia Desert Grassland (15.62 g m^{-2} yr⁻¹) (Wang et al., 2018; Zhou et al., 2020; Ma et al., 2021). These differences were attributed to various factors such as afforestation tree species, tree growth rate, afforestation density, decomposition rate, forest age, management, and protection measures, and soil properties of different locations (Fa et al., 2015; He et al., 2021; Ma et al., 2021; Zhang et al., 2021a). Therefore, it is imperative to investigate the carbon sequestration rate, processes, and regulation mechanisms of typical sand fixation and afforestation in different climate regions. Additionally, valuable support can be provided for the planning and design of carbon sequestration forests by developing afforestation models that promote carbon sequestration, with a focus on managing degraded artificial forests in desert areas, establishing long-term mechanisms for forest management and protection, reducing forest mortality rates, and collaborating on the development of characteristic forest and grass germplasm resources.

3.3. Effect of precipitation on CO₂ flux in the artificial shelter forest

Precipitation directly affects desert soil moisture, soil

microorganisms, plant photosynthesis, and plant roots, leading to complex fluctuations in CO₂ flux within desert ecosystems (Cable et al., 2004; Hao et al., 2010; Ma et al., 2012; Fa et al., 2015; Liu et al., 2015; Zhou et al., 2020). To understand how different precipitation levels influence CO₂ flux in the artificial shelter forest, we analyzed the temporal variation in daily CO₂ flux under varying precipitation levels. We selected 22 precipitation data points greater than 0.1 mm from June to August, which included five consecutive multiday precipitation events. Then, we merged the data for each of the five consecutive precipitation events, resulting in 13 events for analysis. Because the artificial shelter forest received regular drip irrigation, data from days during and after watering were excluded. The daily total CO2 flux remained relatively unchanged compared to sunny weather days, when precipitation amounts were less than 2 mm (Fig. 5). However, at precipitation levels of approximately 4 mm, the artificial shelter forest was stimulated to enhance

 CO_2 absorption within two days after rainfall, with a return to non-precipitation levels within three to four days. For precipitation greater than 8 mm, the impact on the CO_2 budget of the artificial shelter forest became more complex, and displayed volatile changes.

Based on these results, we selected four typical precipitation events of different magnitudes for a more detailed examination (Fig. 6): a 2 mm precipitation event on 19 July 2018 (Figs. 6a and b); a 3.2 mm precipitation event on 13 August 2018 (Figs. 6c and d); a 9.3 mm precipitation event during 22–25 June 2018 (Figs. 6e and f), which consisted of individual events with rainfall amounts of 0.7, 2.9, 2.5 and 3.2 mm over four consecutive days; and a 10.2 mm precipitation event on 9 June 2019 (Figs. 6g and h). The analysis revealed that the 2 mm precipitation event had no effect on the total daily CO₂ flux of the artificial shelter forest (Fig. 6b). The 3.2 mm precipitation event improved the carbon sequestration capacity of the artificial shelter forest, but

Table 2. Total monthly carbon sequestration rates (units: $g m^{-2} month^{-1}$) in the study area during the 2018 and 2019 growing seasons in the artificial shelter forest.

Year	Apr	May	Jun	Jul	Aug	Sep	Oct	Total for the year
2018	-77.55	-124.6	-160.99	-191.73	-187.18	NAN	-40.18	-782.23
2019	-82.98	-220.49	-202.36	-200.99	-136.56	-153.06	-68.63	-1065.07

NAN, no data.

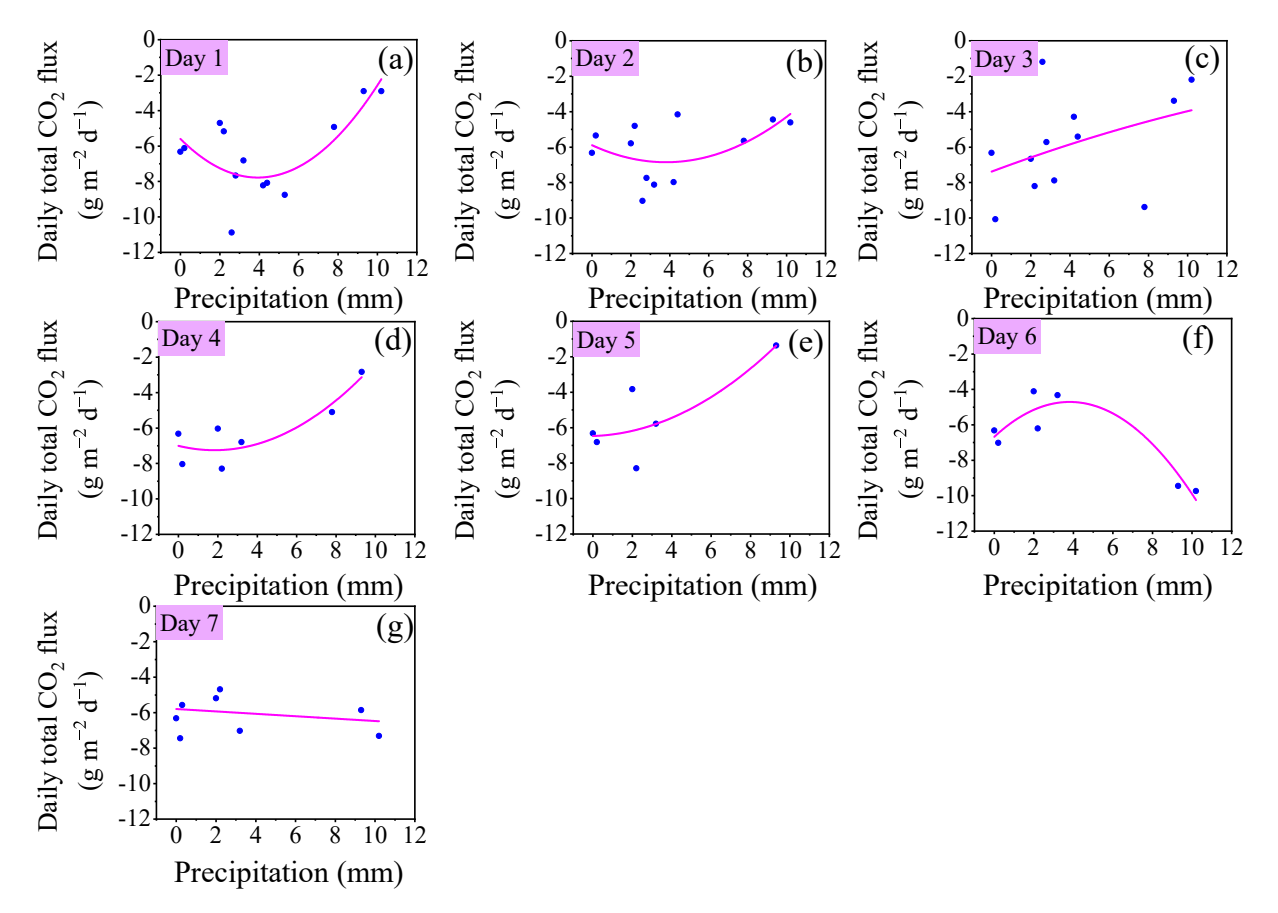


Fig. 5. Variation in daily CO_2 exchange in the artificial shelter forest over time under different precipitation levels. Panels (a) to (g) show the results on days 1–7 after precipitation, respectively.

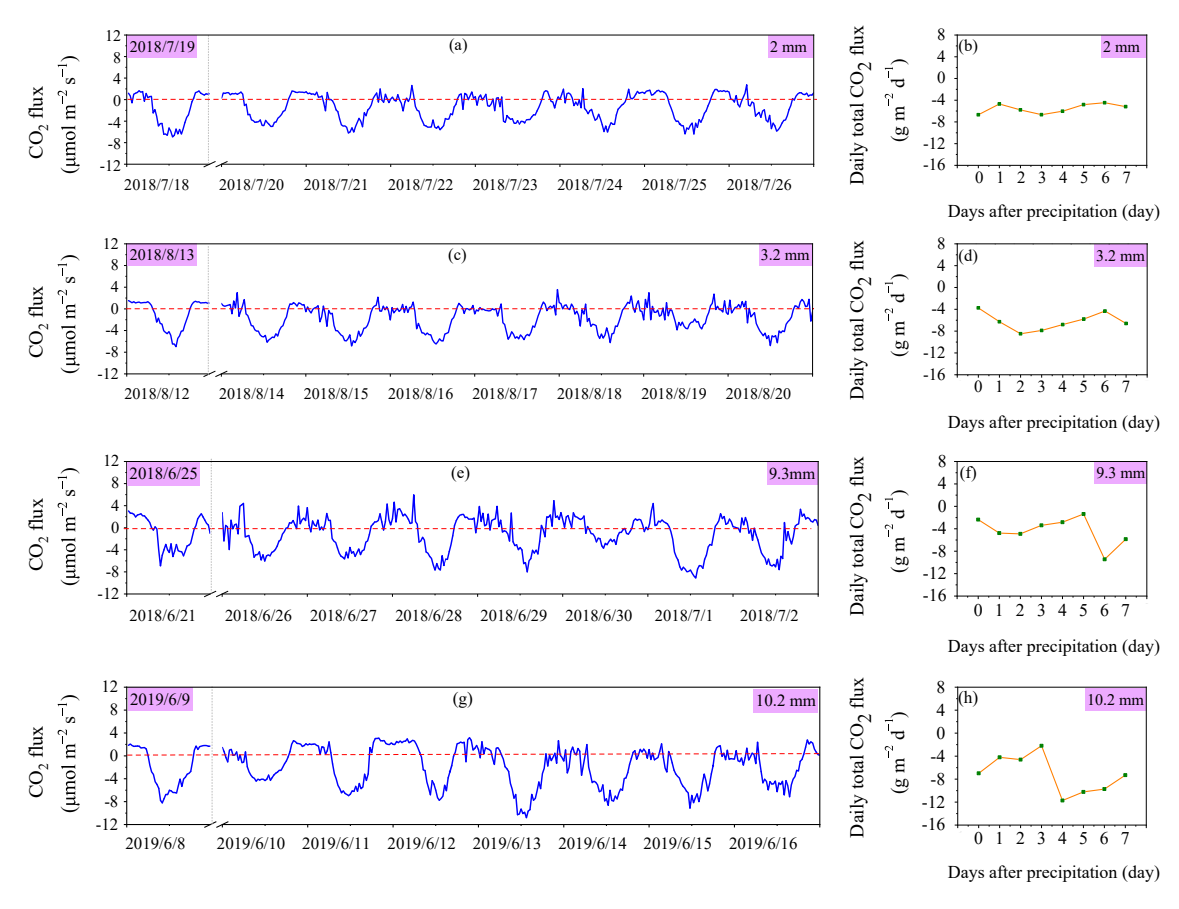


Fig. 6. Half-hourly changes in CO_2 flux and daily total CO_2 exchange on the day before precipitation and 1–7 days after precipitation for precipitation events of different magnitudes: (a, b) 2 mm; (c, d) 3.2 mm; (e, f) 9.3 mm; (g, h) 10.2 mm. The 0 value of the abscissa in the daily total CO_2 exchange graph represents the daily total CO_2 exchange on the day before precipitation.

only for approximately 3 days (Fig. 6d). The 9.3 and 10.2 mm precipitation events affected the daily total CO₂ flux of the artificial shelter forest for approximately 7 days (Fig. 6f). The carbon sequestration capacity of the artificial shelter forest underwent an initial inhibition, followed by a sudden enhancement, and eventually returned gradually to its original state. During the 9.3 mm precipitation event, which consisted of four consecutive precipitation days, the first two days with 3.6 mm of precipitation resulted in a weak enhancement of the carbon sink of the artificial shelter forest. In contrast, heavy precipitation during the 10.2 mm precipitation event initially led to a suppression of the carbon sink (Fig. 6h).

3.4. Relationship between CO₂ flux in the artificial shelter forest and environmental conditions after precipitation

To fully understand the response of CO₂ flux in the shelter forest to precipitation events of varying magnitudes, we conducted a comprehensive analysis using CO₂ flux data one day before and 1–7 days after the 3.2 and 10.2 mm precipitation events, as well as synchronized photosynthetically active radiation (PAR), vapor pressure deficit (VPD), soil respiration, and soil moisture (Figs. 7 and 8). For the 3.2 mm precipitation event, precipitation caused a significant increase

in soil moisture only at a depth of 5 cm (Fig. 7e), with no significant change in soil moisture at 10 cm. This result indicated that a precipitation event of this magnitude only slightly improved the surface soil moisture, with no impact on soil respiration; this moisture was not used by plants with deeper roots in the artificial shelter forest (Yang et al., 2023). However, the carbon sink capacity of the artificial shelter forest was significantly enhanced when PAR remained relatively high and VPD was low within the first 3 days after the precipitation event (Fig. 7c). Consequently, a precipitation event of this magnitude improved the carbon sequestration capacity of the artificial shelter forest by swiftly reducing the VPD, promoting stomatal opening, and enhancing photosynthesis.

In the 7 days after the 10.2 mm precipitation event, except for a significant decrease on 12 June due to cloudy weather, the PAR values remained high (Fig. 8b). This precipitation event resulted in a significant increase in soil moisture at a depth of 10 cm, indicating that water infiltration reached a depth of 10–20 cm in the soil (Fig. 8e). Water at this depth was not used by plants with deep roots in the artificial shelter forest, but significantly stimulated surface soil respiration to promote CO_2 release (Fig. 8d). During the first four days following precipitation, except for the third day when heavy weather conditions led to a decrease in PAR,

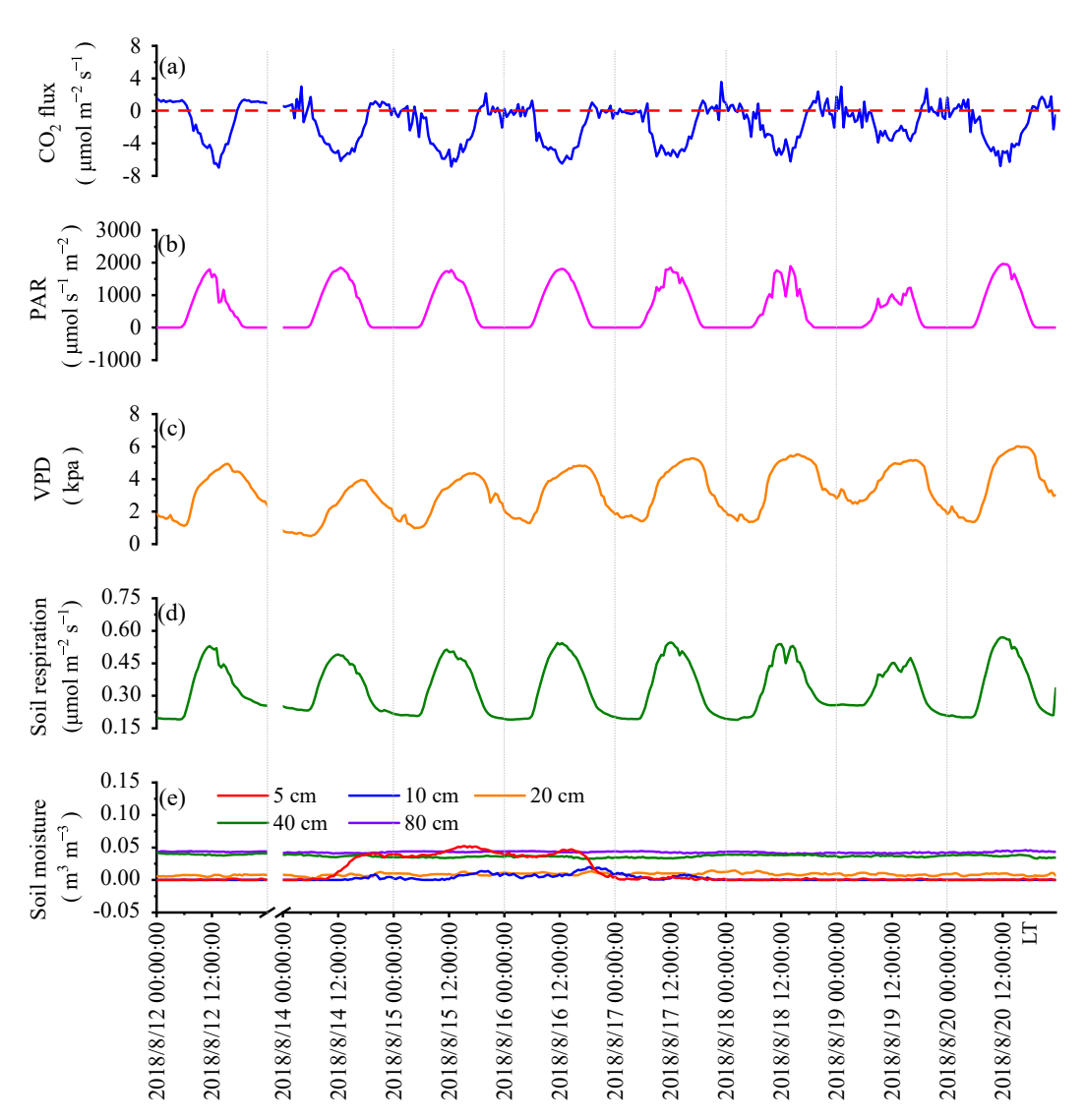


Fig. 7. Variation in CO_2 flux and environmental factors over time in the artificial shelter forest on the day before and within 7 days after a 3.2 mm precipitation event: (a) CO_2 flux; (b) PAR; (c) VPD; (d) soil respiration; and (e) soil moisture at different depths.

the reduction in VPD promoted stomatal opening in plants and enhanced photosynthesis (Figs. 8c and 9c). However, the sudden increase in soil moisture stimulated the recovery of soil dormant microorganisms and the movement of organic substrates, which enhanced soil respiration leading to the release of CO₂ (Yang et al., 2023). In the dynamic equilibrium of soil respiration and photosynthesis stimulated by precipitation, the soil moisture at 5 cm exhibits a clear threshold, which can serve as a good indicator to reflect the strength of precipitation's stimulation on both processes (Fig. 9h). When the soil moisture at 5 cm after precipitation exceeds 0.12 m³ m⁻³, the enhancement of soil respiration caused by precipitation overshadows the increase in photosynthesis. When the soil moisture at 5 cm falls below 0.12 m³ m⁻³, the enhancement of photosynthesis is more than soil respiration. To elucidate the influence of VPD and soil moisture on CO₂ flux, we conducted a segmented regression analysis of VPD and CO2 flux under conditions where

the 5 cm soil moisture content was above and below 0.12 m³ m⁻³ (Fig. 9g). The analysis revealed two distinct CO₂ flux patterns at lower VPD levels. The characteristic of the first pattern was that the shelter forest with low soil moisture had higher carbon sequestration capacity, with a daily carbon sequestration reaching up to 12 g m⁻². The second pattern showed that the overall carbon sequestration capacity of protective forests was lower under higher soil moisture conditions. The enhanced soil respiration caused by high soil moisture during this process effectively offsets the partial absorption of CO₂ caused by enhanced photosynthesis, weakening the carbon sequestration capacity of the entire artificial shelter forest during this period. With the gradual decrease in soil moisture, the weakened soil respiration highlighted enhanced photosynthesis, leading to a sudden increase in the carbon sequestration capacity of the entire artificial shelter forest. Finally, the ability of the artificial shelter forest to absorb CO₂ gradually recovered to the state before precipita-

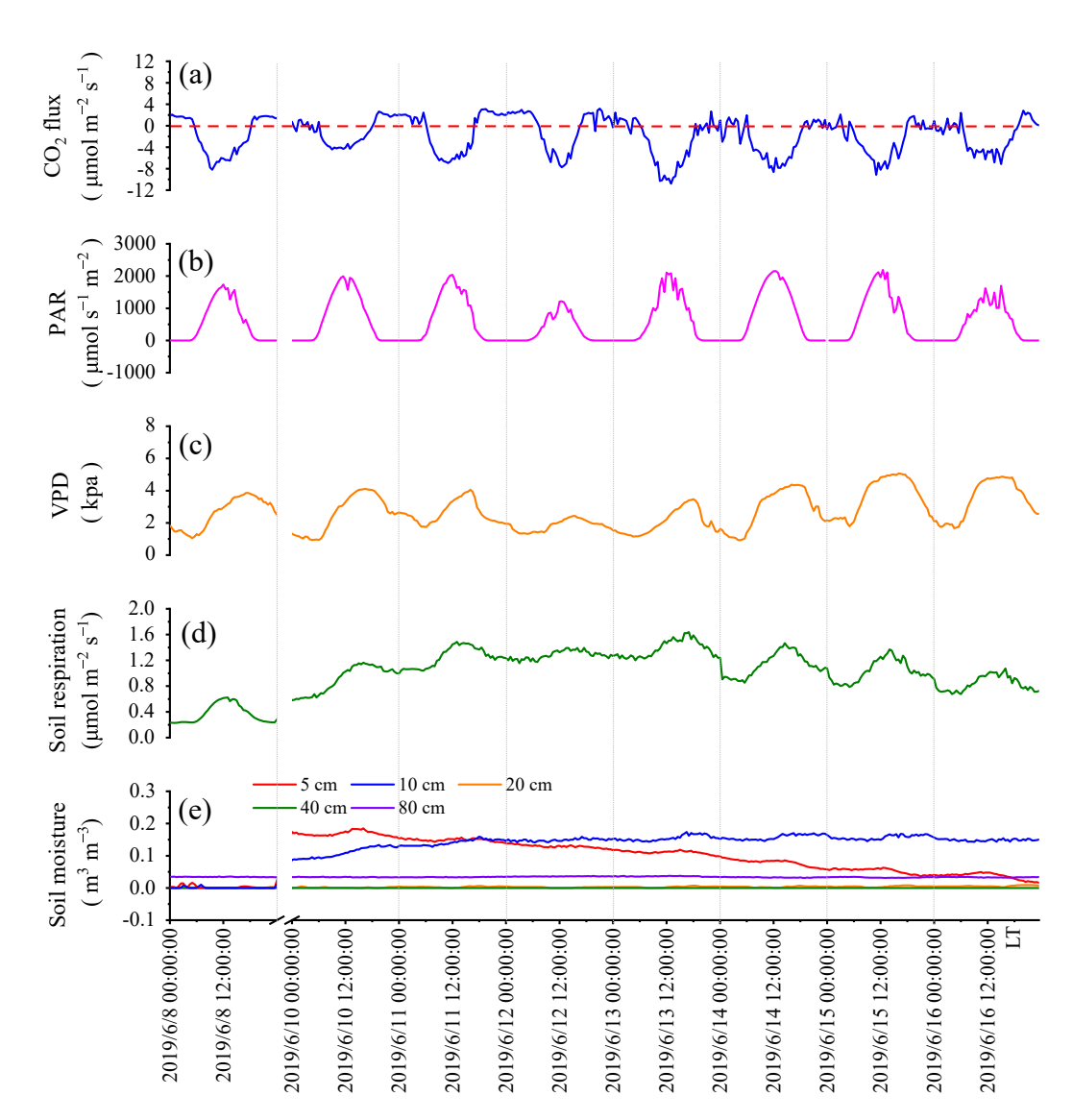


Fig. 8. Variation in CO_2 flux and environmental factors over time in the artificial shelter forest on the day before and within 7 days after a 10.2 mm precipitation event: (a) CO_2 flux; (b) PAR; (c) VPD; (d) soil respiration; and (e) soil moisture at different depths.

tion. Yang et al. (2021) also found that in the Badain Jaran Desert, the precipitation magnitude had variable effects on the desert ecosystem; as the precipitation intensity increased, the residual time of the precipitation influence was extended. However, we identified a unique phenomenon, in which precipitation greater than 8 mm first inhibited and then promoted the CO_2 absorption capacity of artificial shelter forest.

4. Conclusion

The CO₂ flux of an artificial shelter forest in an arid environment in the hinterland of the Taklimakan Desert was monitored from 2018 to 2019 using an eddy covariance system. The impact of establishing an artificial shelter forest on the carbon sequestration capacity of the desert was analyzed and the forest response mechanism to precipitation events of varying magnitudes was determined. The results demon-

strated that the establishment of the artificial shelter forest in the desert increased the carbon storage capacity of the ecosystem approximately 140-fold by combining the original inorganic carbon sequestration process with plant photosynthesis. The artificial shelter forest absorbed approximately 1000 g m⁻² of CO₂ every year, which improved the regional ecological environment and transformed the desert into a significant terrestrial carbon sink.

The carbon sequestration capacity of the artificial shelter forest responded differently to precipitation events of varying magnitudes. Precipitation less than 2 mm was rapidly evaporated within a short period of time and did not alleviate long-term drought in the desert environment. Therefore, precipitation of this magnitude had little impact on the carbon sink capacity of the artificial shelter forest. Precipitation events of 3–6 mm increased the atmospheric humidity and caused a temporary decline in VPD, thereby promoting photosynthesis and strengthening the carbon sequestration capacity of

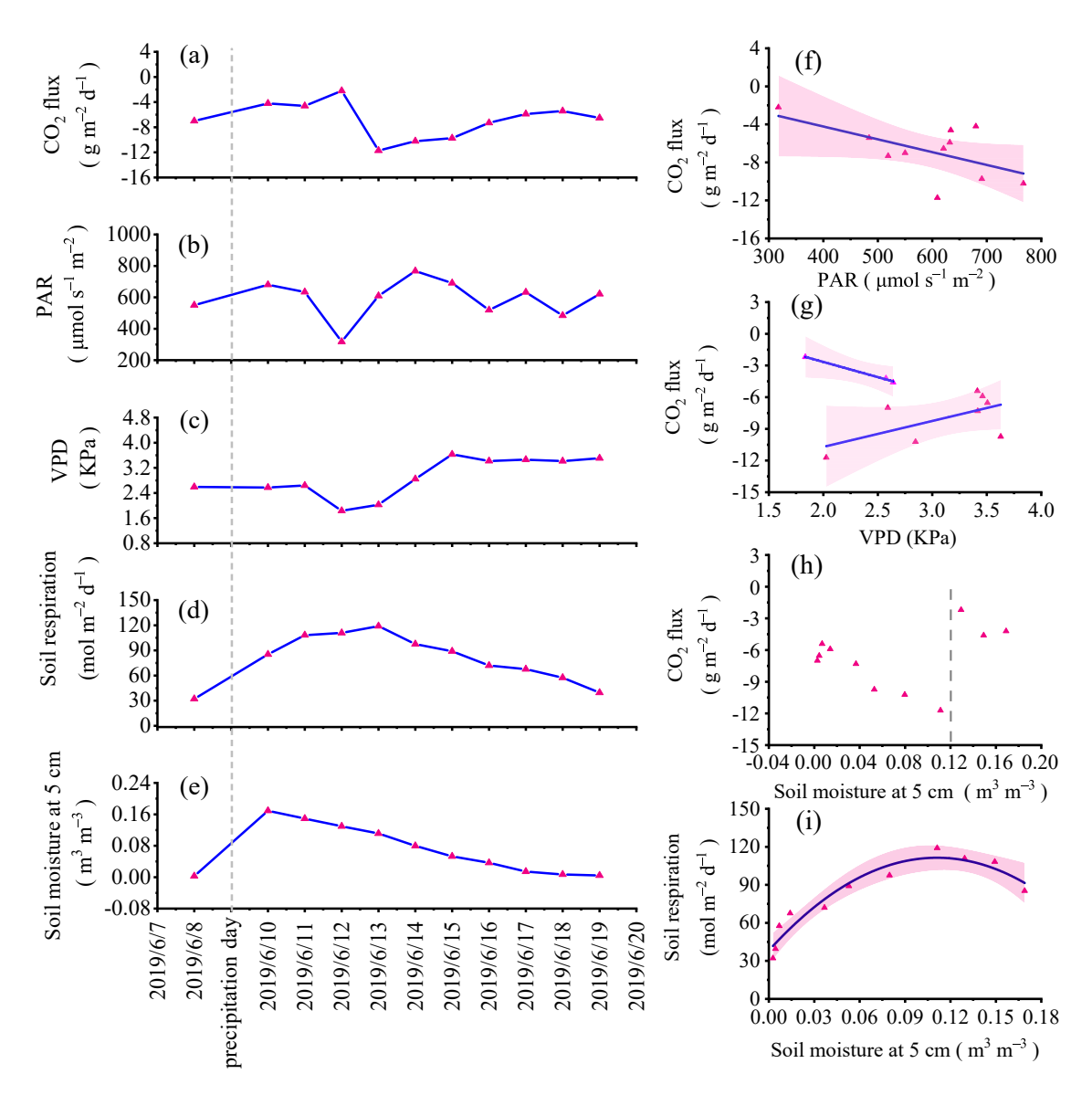


Fig. 9. The changes in various environmental factors and the relationship between environmental factors of the artificial shelter forest from moist to dry after 10.2 mm precipitation: (a) CO₂ flux; (b) PAR; (c) VPD; (d) soil respiration; (e) soil moisture at 5 cm. The regression relationship between (f) PAR, (g) VPD, (h) soil moisture at 5 cm, and CO₂ flux. (i) The regression relationship between soil respiration and soil moisture at 5 cm.

the artificial shelter forest. However, because this amount of precipitation only wetted the soil surface, and thus evaporated completely within 3 days, the duration of the enhancement of the absorption of CO₂ by the artificial shelter forest after rainfall was relatively short. Precipitation greater than 8 mm promoted an increase in soil moisture, which in turn stimulated microbial decomposition and organic matter transport, leading to a significant increase in soil respiration within the first few days after precipitation, and offsetting part of the increase in photosynthesis. In the dynamic equilibrium of soil respiration and photosynthesis stimulated by precipitation, the soil moisture at 5 cm exhibits a clear threshold, which can serve as a good indicator to reflect the strength of precipitation's stimulation on both processes. When the soil moisture at 5 cm after precipitation exceeds 0.12 m³ m⁻³, the enhancement of soil respiration caused by precipitation

overshadows the increase in photosynthesis. When the soil moisture at 5 cm falls below 0.12 m³ m⁻³, the enhancement of photosynthesis caused by precipitation than that of soil respiration. As a result, the overall carbon sequestration capacity of the artificial shelter forest shows a decreasing trend followed by an increasing trend. These findings provide data support for efforts to quantify the contribution of artificial afforestation to carbon sequestration and sink enhancement in arid areas, and will contribute to the formulation and implementation of management measures for artificial forests in desert environments.

Acknowledgements. This work was jointly supported by the Natural Science Foundation of Xinjiang Uygur Autonomous Region (Grant No. 2022D01E104), the National Natural Science Foundation General Project (Grant No. 41975010), the China Post-

doctoral Science Foundation (Grant No. 2022MD723851), and the Scientific and Technological Innovation Team (Tianshan Innovation Team) project (Grant No. 2022TSYCTD0007).

REFERENCES

- Ai, M. M., Y. Y. Sun, B. Yan, and Y. Wei, 2018: A summary of the impact of land degradation on soil carbon sequestration. *IOP Conference Series: Materials Science and Engineering*, 394, 052028, https://doi.org/10.1088/1757-899X/394/5/ 052028.
- Aubinet, M., B. Heinesch, and B. Longdoz, 2002: Estimation of the carbon sequestration by a heterogeneous forest: Night flux corrections, heterogeneity of the site and inter-annual variability. *Global Change Biology*, **8**(11), 1053–1071, https://doi.org/10.1046/j.1365-2486.2002.00529.x.
- Baldocchi, D. D., 2003: Assessing the eddy covariance technique for evaluating carbon dioxide exchange rates of ecosystems: Past, present and future. *Global Change Biology*, **9**, 479–492, https://doi.org/10.1046/j.1365-2486.2003.00629.x.
- Cable, J. M., and T. E. Huxman, 2004: Precipitation pulse size effects on Sonoran Desert soil microbial crusts. *Oecologia*, 141(2), 317–324, https://doi.org/10.1007/s00442-003-1461-7.
- Donat, M. G., A. L. Lowry, L. V. Alexander, P. A. O'Gorman, and N. Maher, 2017: Addendum: More extreme precipitation in the world's dry and wet regions. *Nature Climate Change*, 7(2), 154–158, https://doi.org/10.1038/nclimate3160.
- Duan, Z. H., H. L. Xiao, Z. B. Dong, X. D. He, and G. Wang, 2001: Estimate of total CO₂ output from desertified sandy land in China. *Atmos. Environ.*, **35**(34), 5915–5921, https://doi.org/10.1016/S1352-2310(01)00406-X.
- Fa, K.-Y., J.-B. Liu, Y.-Q. Zhang, B. Wu, S.-G. Qin, W. Feng, and Z.-R. Lai, 2015: CO₂ absorption of sandy soil induced by rainfall pulses in a desert ecosystem. *Hydrological Processes*, 29(8), 2043–2051, https://doi.org/10.1002/hyp.10350.
- Falge, E., and Coauthors, 2001: Gap filling strategies for defensible annual sums of net ecosystem exchange. *Agricultural and Forest Meteorology*, **107**, 43–69, https://doi.org/10.1016/S0168-1923(00)00225-2.
- Gong, Z. L., Y. Tang, W. L. Xu, and Z. S. Mou, 2019: Rapid sequestration of ecosystem carbon in 30-year reforestation with mixed species in dry hot valley of the Jinsha River. *International Journal of Environmental Research and Public Health*, 16(11), 1937, https://doi.org/10.3390/ijerph1611
- Hao, Y. B., Y. F. Wang, X. R. Mei, X. Y. Cui, X. Q. Zhou, and X. Z. Huang, 2010: The sensitivity of temperate steppe CO₂ exchange to the quantity and timing of natural interannual rainfall. *Ecological Informatics*, 5(3), 222–228, https://doi.org/10.1016/j.ecoinf.2009.10.002.
- Hastings, S. J., W. C. Oechel, and A. Muhlia-Melo, 2005: Diurnal, seasonal and annual variation in the net ecosystem CO₂ exchange of a desert shrub community (Sarcocaulescent) in Baja California, Mexico. *Global Change Biology*, 11(6): 927–939, https://doi.org/10.1111/j.1365-2486.2005.00951.x.
- He, L. X. Z., Z. Q. Jia, Q. X. Li, Y. Y. Zhang, R. N. Wu, J. Dai, and Y. Gao, 2021: Fine root dynamic characteristics and effect on plantation's carbon sequestration of three *Salix* shrub plantations in Tibetan Plateau alpine sandy land. *Ecology and Evolution*, **11**(6), 2645–2659, https://doi.org/10.

- 1002/ece3.7221.
- Huang, J., and Coauthors, 2017: Dryland climate change: Recent progress and challenges. *Rev. Geophys.*, **55**, 719–778, https://doi.org/10.1002/2016RG000550.
- Huang, J. P., H. P. Yu, X. D. Guan, G. Y. Wang, and R. X. Guo, 2016a: Accelerated dryland expansion under climate change. *Nature Climate Change*, **6**(2), 166–172, https://doi.org/10.1038/nclimate2837.
- Huang, J. P., M. X. Ji, Y. K. Xie, S. S. Wang, Y. L. He, and J. J. Ran, 2016b: Global semi-arid climate change over last 60 years. *Climate Dynamics*, 46, 1131–1150, https://doi.org/10.1007/s00382-015-2636-8.
- Huang, J. P., J. R. Ma, X. D. Guan, Y. Li, and Y. L. He, 2019: Progress in semi-arid climate change studies in China. *Adv. Atmos. Sci.*, 36(9), 922–937, https://doi.org/10.1007/s00376-018-8200-9.
- Lal, R., 2004: Carbon sequestration in Dryland ecosystems. *Environmental Management*, **33**(4), 528–544, https://doi.org/10.1007/s00267-003-9110-9.
- Lei, J. Q., and Coauthors, 2008: Comprehensive eco-environmental effects of the shelter-forest ecological engineering along the Tarim Desert Highway. *Chinese Science Bulletin*, **53**(S2), 190–202, https://doi.org/10.1007/s11434-008-6022-3.
- Li, B. F., Y. N. Chen, Z. S. Chen, H. G. Xiong, and L. S. Lian, 2016: Why does precipitation in Northwest China show a significant increasing trend from 1960 to 2010. *Atmospheric Research*, 167, 275–284, https://doi.org/10.1016/j.atmosres. 2015.08.017.
- Li, C. J., J. Q. Lei, Y. Zhao, X. W. Xu, and S. Y. Li, 2015: Effect of saline water irrigation on soil development and plant growth in the Taklimakan Desert Highway shelterbelt. *Soil and Tillage Research*, **146**, 99–107, https://doi.org/10.1016/j.still.2014.03.013.
- Liang, X. Y., P. F. Li, J. L. Wang, F. K. Shun Chan, C. Togtokh, A. Ochir, and D. Davaasuren, 2021: Research progress of desertification and its prevention in Mongolia. *Sustainability*, 13(12), 6861, https://doi.org/10.3390/su13126861.
- Liu, J.-B., Y.-Q. Zhang, B. Wu, S.-G. Qin, X. Jia, K.-Y. Fa, W. Feng, and Z.-R. Lai, 2015: Effect of vegetation rehabilitation on soil carbon and its fractions in Mu Us Desert, Northwest China. *International Journal of Phytoremediation*, 17(6), 529–537, https://doi.org/10.1080/15226514.2014.922923.
- Liu, W. H., J. J. Zhu, Q. Q. Jia, X. Zheng, J. S. Li, X. D. Lou, and L. L. Hu, 2014: Carbon sequestration effects of shrublands in Three-North Shelterbelt Forest Region, China. *Chinese Geo*graphical Science, 24(4), 444–453, https://doi.org/10.1007/ s11769-014-0698-x.
- Ma, J., X.-J. Zheng, and Y. Li, 2012: The response of CO₂ flux to rain pulses at a saline desert. *Hydrological Processes*, **26**(26), 4029–4037, https://doi.org/10.1002/hyp.9204.
- Ma, Q. L., X. Y. Wang, F. Chen, L. Y. Wei, D. K. Zhang, and H. J. Jin, 2021: Carbon sequestration of sand-fixing plantation of *Haloxylon ammodendron* in Shiyang River Basin: Storage, rate and potential. *Global Ecology and Conservation*, 28, e01607, https://doi.org/10.1016/j.gecco.2021.e01607.
- Martínez-Valderrama, J., Ibáñez, J., Del Barrio, G., M. E. Sanjuán, F. J. Alcalá, S. Martínez-Vicente, A. Ruiz, and J. Puigdefábregas, 2016: Present and future of desertification in Spain: Implementation of a surveillance system to prevent land degradation. Science of the Total Environment, 563–564, 169–178, https://doi.org/10.1016/j.scitotenv.2016.04.065.

- Midgley, G. F., J. N. Aranibar, K. B. Mantlana, and S. Macko, 2004: Photosynthetic and gas exchange characteristics of dominant woody plants on a moisture gradient in an African savanna. *Global Change Biology*, **10**(3), 309–317, https://doi.org/10.1111/j.1365-2486.2003.00696.x.
- Reynolds, J. F., R. A. Virginia, P. R. Kemp, A. G. De Soyza, and D. C. Tremmel, 1999: Impact of drought on desert shrubs: Effects of seasonality and degree of resource island development. *Ecological Monographs*, **69**(1), 69–106, https://doi.org/10.1890/0012-9615(1999)069[0069:IODODS]2.0.CO;2.
- Reynolds, J. F., and Coauthors, 2007: Global desertification: Building a science for dryland development. *Science*, **316**(5826), 847–851, https://doi.org/10.1126/science.1131634.
- Shen, Y. J., C. M. Liu, M. Liu, Y. Zeng, and C. Y. Tian, 2010: Change in pan evaporation over the past 50 years in the arid region of China. *Hydrological Processes*, **24**(2), 225–231, https://doi.org/10.1002/hyp.7435.
- Wang, H. F., J. Q. Lei, S. Y. Li, J. L. Fan, Y. G. Li, S. G. Sun, and Q. Chang, 2008: Effect of the shelterbelt along the Tarim desert highway on air temperature and humidity. *Chinese Science Bulletin*, 53, 41–52, https://doi.org/10.1007/s11434-008-6004-5.
- Wang, S. Q., and Y. Huang, 2020: Determinants of soil organic carbon sequestration and its contribution to ecosystem carbon sinks of planted forests. *Global Change Biology*, 26(5), 3163–3173, https://doi.org/10.1111/gcb.15036.
- Wang, Y. H., J. Chen, G. S. Zhou, C. L. Shao, J. Chen, Y. Wang, and J. M. Song, 2018: Predominance of precipitation event controls ecosystem CO₂ exchange in an Inner Mongolian desert grassland, China. *Journal of Cleaner Production*, 197, 781–793, https://doi.org/10.1016/j.jclepro.2018.06.107.
- Wijitkosum, S., 2021: Factor influencing land degradation sensitivity and desertification in a drought prone watershed in Thailand. *International Soil and Water Conservation Research*, **9**, 217–228, https://doi.org/10.1016/j.iswcr.2020.10.005.
- Xu, D. Y., A. L. Song, D. J. Li, X. Ding, and Z. Y. Wang, 2019: Assessing the relative role of climate change and human activities in desertification of North China from 1981 to 2010. Frontiers of Earth Science, 13(1), 43–54, https://doi.org/10.1007/s11707-018-0706-z.
- Yang, F., M. Ali, X. Q. Zheng, Q. He, X. H. Yang, W. Huo, F. C. Liang, and S. M. Wang, 2017: Diurnal dynamics of soil respiration and the influencing factors for three land-cover types in the hinterland of the Taklimakan Desert, China. *Journal of Arid Land*, **9**(4), 568–579, https://doi.org/10.1007/s40333-017-0060-0.
- Yang, F., and Coauthors, 2020a: Impact of differences in soil temperature on the desert carbon sink. *Geoderma*, **379**, 114636, https://doi.org/10.1016/j.geoderma.2020.114636.

- Yang, F., and Coauthors, 2020b: Taklimakan desert carbon-sink decreases under climate change. *Science Bulletin*, **65**(6), 431–433, https://doi.org/10.1016/j.scib.2019.12.022.
- Yang, F., and Coauthors, 2021: Desert environment and climate observation network over the Taklimakan Desert. *Bull. Amer. Meteor. Soc.*, **102**(6), E1172–E1191, https://doi.org/ 10.1175/BAMS-D-20-0236.1.
- Yang, F., and Coauthors, 2023: Desert abiotic carbon sequestration weakening by precipitation. *Environmental Science & Technology*, 57, 7174–7184, https://doi.org/10.1021/acs.est. 2c09470
- Yang, P., L. Q. Zhao, X. R. Liang, Z. M. Niu, H. Zhao, Y. Y. Wang, and N. Wang, 2022: Response of net ecosystem CO₂ exchange to precipitation events in the Badain Jaran desert. Environmental Science and Pollution Research, 29, 36 486–36 501, https://doi.org/10.1007/s11356-021-18229-0.
- Yao, J. Q., Y. N. Chen, J. Chen, Y. Zhao, D. Tuoliewubieke, J. G. Li, L. M. Yang, and W. Y. Mao, 2020: Intensification of extreme precipitation in arid central Asia. *J. Hydrol.*, 598, 125760, https://doi.org/10.1016/j.jhydrol.2020.125760.
- Zhang, Q., J. H. Yang, W. Wang, P. L. Ma, G. Y. Lu, X. Y. Liu, H. P. Yu, and F. Fang, 2021b: Climatic warming and humidification in the arid region of Northwest China: Multi-scale characteristics and impacts on ecological vegetation. *Journal of Meteorological Research*, 35(1), 113–127, https://doi.org/ 10.1007/s13351-021-0105-3.
- Zhang, Y., Y.-Z. Xie, H.-B. Ma, J. Zhang, L. Jing, Y.-T. Wang, and J.-P. Li, 2021a: The responses of soil respiration to changed precipitation and increased temperature in desert grassland in northern China. *Journal of Arid Environments*, 193, 104579, https://doi.org/10.1016/j.jaridenv.2021. 104579.
- Zhang, Z. H., and D. Huisingh, 2018: Combating desertification in China: Monitoring, control, management and revegetation. *Journal of Cleaner Production*, 182, 765–775, https:// doi.org/10.1016/j.jclepro.2018.01.233.
- Zhang, Z.-S., X.-R. Li, L.-C. Liu, R.-L. Jia, J.-G. Zhang, and T. Wang, 2009: Distribution, biomass, and dynamics of roots in a revegetated stand of *Caragana korshinskii* in the Tengger Desert, northwestern China. *Journal of Plant Research*, 122(1), 109–119, https://doi.org/10.1007/s10265-008-0196-2.
- Zhou, Y. Y., X. R. Li, Y. H. Gao, M. Z. He, M. M. Wang, Y. L. Wang, L. N. Zhao, and Y. F. Li, 2020: Carbon fluxes response of an artificial sand-binding vegetation system to rainfall variation during the growing season in the Tengger Desert. *Journal of Environmental Management*, 266, 110556, https://doi.org/10.1016/j.jenvman.2020.110556.